

# Scalable Manufacturing of Hierarchical Nanostructures for Thermal Management

by

Christopher J. Love

B.S. Chemistry  
Massachusetts Institute of Technology, 2009

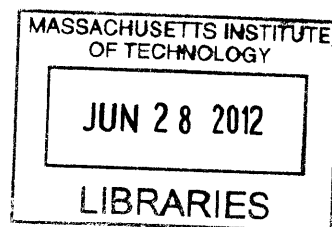
SUBMITTED TO THE DEPARTMENT OF MECHANICAL ENGINEERING IN  
PARTIAL FULFILLMENT OF THE REQUIREMENTS FOR THE DEGREE OF

MASTER OF SCIENCE IN MECHANICAL ENGINEERING  
AT THE  
MASSACHUSETTS INSTITUTE OF TECHNOLOGY

JUNE 2012

©2012 Christopher J. Love. All rights reserved.

**ARCHIVES**



The author hereby grants to MIT permission to reproduce and to distribute publicly paper  
and electronic copies of this thesis document in whole or in part in any medium now  
known or hereafter created.

Signature of Author: \_\_\_\_\_  
Department of Mechanical Engineering  
May 11, 2012

Certified by: \_\_\_\_\_  
Kripa K. Varanasi  
Doherty Chair in Ocean Utilization  
Associate Professor of Mechanical Engineering  
Thesis Supervisor

Accepted by: \_\_\_\_\_  
David E. Hardt  
Ralph E. and Eloise F. Cross Professor of Mechanical Engineering  
Graduate Officer



# Scalable Manufacturing of Hierarchical Nanostructures for Thermal Management

by

Christopher J. Love

Submitted to the Department of Mechanical Engineering on May 11, 2012 in Partial  
Fulfillment of the Requirements for the Degree of Master of Science in  
Mechanical Engineering

## ABSTRACT

The focus of this thesis is a new *simple and scalable* process to make surface coatings that have multiple length scales, or hierarchical features. Typically, the formation of hierarchical structures involves multiple steps and/or long processing times. In this new process, the hierarchical geometry is formed in a single step. The starting material—spherical copper powder—is oxidized in ambient air. Depending on the starting size of the powder, copper oxide nanowires may or may not form. Systematic thermogravimetric analysis (TGA) and in-situ x-ray diffraction (XRD) studies provide insights into the size-dependent thermal oxidation process. The proposed mechanism is supported by another interesting geometrical transformation: in the same single-step process, a large void is formed in the particles. The tunable nanowire growth is used to make new kinds of hierarchical coatings with *enhanced heat-transfer performance in spray-cooling applications*, which include nuclear reactor boiling, continuous casting of metals, and thermal management of electronics.

Thesis Supervisor: Kripa K. Varanasi  
Title: Doherty Chair in Ocean Utilization  
Associate Professor of Mechanical Engineering



## **ACKNOWLEDGEMENTS**

I am thankful for the many blessings and opportunities I have been given.

I thank J. David Smith and Yuehua Cui, my labmates who worked with me on various aspects of the scalable manufacturing process. I thank HyukMin Kwon, another labmate who worked with me on the spray-cooling experiments. I am grateful to my thesis advisor, Professor Kripa Varanasi, whose motivation, creativity, and friendship keep me on track to realize my goals as a graduate student and beyond. I thank all of my other labmates for stimulating research discussions and encouragement. I thank the Mechanical Engineering Department and Laboratory for Manufacturing and Productivity for providing me with a great work environment.

I thank my friends and family for their continued support and love. I thank the many mentors and great teachers I've had in my life.

I thank the MIT Energy Initiative and the National Science Foundation for the fellowship funding they awarded me.

## **Table of Contents**

Introduction.....	7
Size-dependent Thermal Oxidation.....	8
Mechanism of Size-Dependent Nanowire Formation.....	10
Experimental Methods .....	17
Applications .....	18
Leidenfrost Experiments.....	20
Conclusion .....	23
Bibliography .....	24

## Introduction

Multi-length scale or hierarchical structures have been suggested to have a favorable geometry for a range of natural [1-4] phenomena, but the formation of synthetic hierarchical structures for other applications generally requires multiple steps and/or long processing times [5, 6]. In addition to limited process scalability, many of the reported hierarchical structures would pose challenges in durability at elevated temperatures and moderate mechanical loading that are common in thermal management, one of the main focus areas of our research group. To improve heat transfer processes, we tailor solid-liquid-vapor interfacial properties with new durable coatings that have optimized material chemistry and surface structures. In these applications, we have previously demonstrated [7-9] that hierarchical structures have favorable geometrical and interfacial properties.

With a particular desire to improve electronics cooling and boiling heat transfer, we started working with copper powder to make new wick structures with tunable thermal, interfacial, and mass transport properties. One common use of a wick structure is in a heat pipe [10], where porous copper powder—sintered in an inert atmosphere—provides the capillary force to passively wick the working fluid back to the evaporator section. Previous research [11, 12] has characterized and optimized heat pipe performance with particle size, porosity, and thickness of the sintered metal structure. In boiling heat transfer, recent pioneering work [13-15] has demonstrated that substantial improvements in the heat transfer coefficient and critical heat flux can be made with new surface structures over standard flat surfaces.

The oxidation of copper foils, grids, and wires has been shown to form copper oxide nanowires in a straightforward manner at temperatures of 400-700°C [16, 17]. Here we report the first study on the thermal oxidation of copper particles. By changing the particle size, we demonstrate for the first time the ability to control the extent of nanowire growth and identify regimes where many nanowires and almost no nanowires form. Systematic thermogravimetric analysis (TGA) and in-situ x-ray diffraction (XRD) experiments of thermal oxidation were conducted on

particles of various sizes to understand the size-dependent process and propose a mechanism for the reaction. Using this new process of tunable nanowire growth, we demonstrate the formation of new hierarchical structures and use them to make new coatings with improved thermal management in spray cooling.

## Size-dependent Thermal Oxidation

Prior to thermal oxidation, copper particles of 1, 10, and 50  $\mu\text{m}$  average size were absent of nanowires (Figure 1a). After thermal treatment in the furnace, all samples were black in color. Characterization on a field emission scanning electron microscope (FESEM, Zeiss Ultra55) revealed nanowire protrusions from spherical particles (Figure 1b). Each nanowire grew approximately perpendicular to the surface, most of the wires were straight, and there was a significant variation in nanowire length. We did not observe branching or entanglement of the nanowires. Based on previous reports [17, 18], we expect the nanowires to be monoclinic  $\text{CuO}$ . The particles were roughened by the thermal oxidation process yielding nanoscale indentations. A comparison of the nanowire coverage on particles of different size for an oxidation temperature of 600°C is shown in Figure 1b and reveals a difference in nanowire growth based on the particle size. We observe a critical size of around 3  $\mu\text{m}$  above which nanowires form, but the transition is stochastic; therefore, we specify two distinct regimes of nanowire growth: particle sizes of around 3  $\mu\text{m}$  and below with no noticeable nanowire coverage and particle sizes of 10  $\mu\text{m}$  and larger with appreciable nanowire coverage. Furthermore, particles with an average size  $\sim 1 \mu\text{m}$  tend to agglomerate and form dense, sintered structures even without prior pressing or packing.



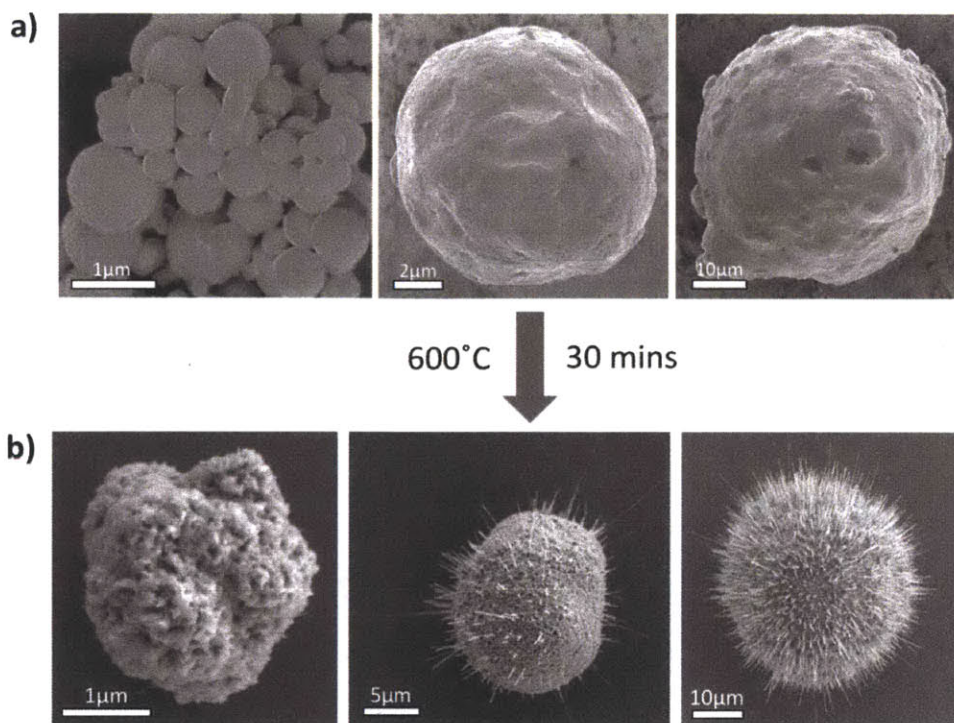


**Figure 1.** Size-Dependent Thermal Oxidation of Copper Particles in Ambient Air. a) As-received, unprocessed copper powder of average diameter 1, 10, and 50μm; b) oxidized 1, 10, 50μm particles with no noticeable nanowire coverage on the smaller 1μm particles and significant nanowire coverage on the larger sizes.

At 400°C and 500°C, we have seen a similar clear transition in nanowire growth on particle sizes between 3-10μm (Figure 2). The influence of temperature on nanowire growth has been noted previously[16]. Within the reported [16, 17] temperature range of 400-700°C of nanowire growth, the effect of temperature was much less pronounced than that of the particle size. Furthermore, we did not observe a consistent trend in nanowire growth with temperature.

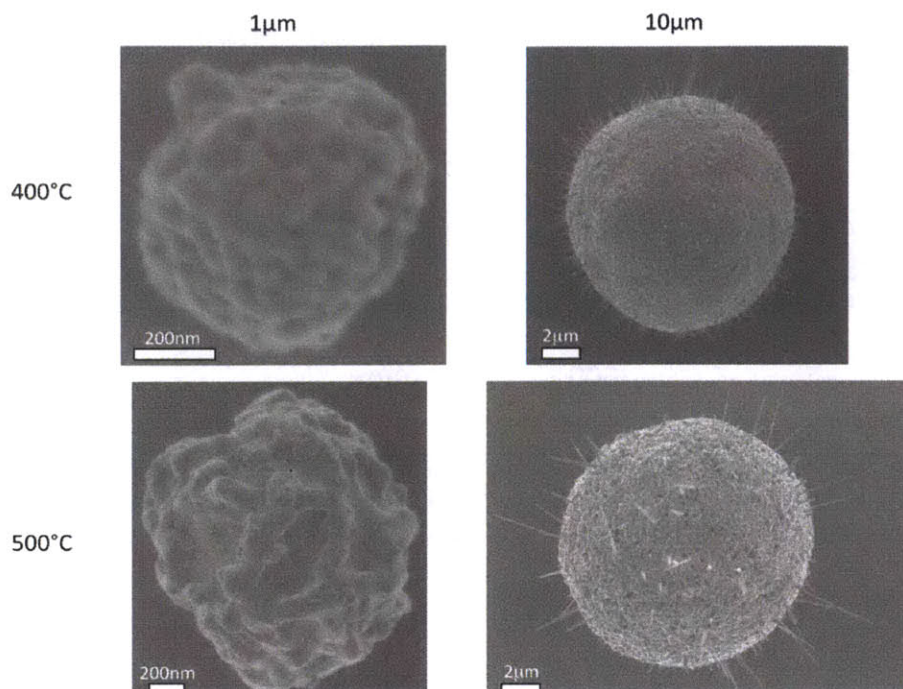


**Figure 2.** SEM images of 1 $\mu\text{m}$  and 10 $\mu\text{m}$  particle sizes at 400°C and 500°C. Similar to our results at 600°C (Figure 1), we observe little to no nanowires on the 1 $\mu\text{m}$  particles, but the larger 10 $\mu\text{m}$  particles are covered by nanowires.

## Mechanism of Size-Dependent Nanowire Formation

The growth mechanism of nanowires by thermal oxidation is not well understood in the literature. Most literature studies have proposed a mechanism of copper oxidation and nanowire growth based on two-steps [16, 17]:

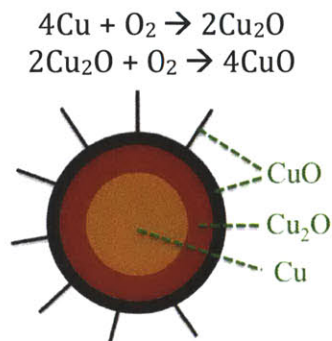


**Figure 3.** Schematic of the two-step oxidation of copper powder.

The growth of nanowires involves the formation of a major product ( $\text{Cu}_2\text{O}$ ) that acts as a precursor to the rate-determining second reaction (Figure 3). X-ray diffraction (XRD) patterns of oxidized copper samples have supported this mechanism by revealing a strong signal for  $\text{Cu}_2\text{O}$  with a much smaller peak corresponding to  $\text{CuO}$  [16, 17]. The  $\text{Cu}_2\text{O}$  layer has been proposed [19] to be a seed for  $\text{CuO}$  nanowire growth. After removal of the  $\text{Cu}_2\text{O}$  phase, no increase in nanowire length and diameter was observed [19] with increasing duration at the same temperature. Furthermore, it has been suggested [20] that the morphology of the outer nanowire “layer” is determined by the microstructure of the underlying  $\text{Cu}_2\text{O}$  layer.

The most recent literature and proposed models suggests two key ideas for nanowire growth to occur: outward copper ion diffusion through a defective  $\text{Cu}_2\text{O}$  layer [20] and a critical compressive stress between  $\text{Cu}_2\text{O}/\text{CuO}$  [18]. Other models [17, 21] involving the evaporation and recondensation of oxide species (vapor-solid model) have not been well-supported [18, 20, 22]. To understand the observed size-dependent behavior and determine if it follows the proposed mechanisms, we monitored bulk oxidation rate by thermogravimetric analysis (TGA Q50, TA Instruments) at  $600^\circ\text{C}$  for 1hr in air. From TGA (Figure 4), we observe that smaller particles undergo oxidation at a much faster rate than larger particles with a consistent trend of increasing rate with decreasing size. As expected, the foil sample has the slowest kinetics. The higher rate of oxidation of the smaller particles is presumably due to their larger specific surface area.

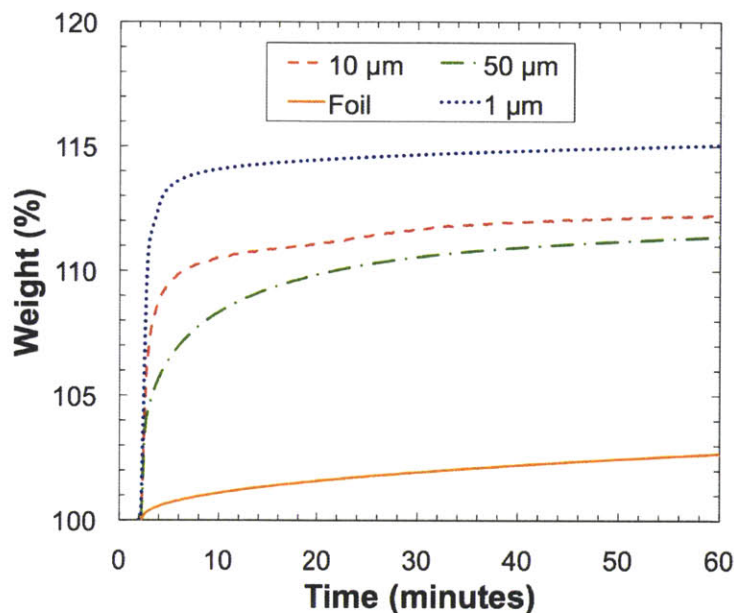


**Figure 4.** Thermogravimetric (TGA) analysis of differently sized copper particles and bulk foil samples oxidized in air at 600°C. As the particle size decreases, the oxidation rate increases. As expected, the bulk foil sample has the slowest kinetics.

In order to further understand the size-dependent results in our SEM and TGA experiments, we examined the evolution of the copper and copper oxide phases with time by conducting a detailed in-situ XRD (PANalytical X'Pert Pro) experiment. The oxidation was conducted at 600°C in an atmosphere consisting of 5% oxygen and 95% nitrogen in order to slow down the rate of the reaction and capture the evolution of the initial process. A Rietveld analysis was performed on the raw data to determine changes in mass percent of each compound, which are shown in Figure 5. For all particle sizes in Figure 5, we observe the expected peaks for Cu, Cu<sub>2</sub>O, and CuO, though considerable difference is seen in the evolution of these compounds based on the size as discussed below.

Our results support the general mechanism of nanowire formation based on the availability of copper ions and an optimal oxide shell. By examining three parameters—copper availability, Cu<sub>2</sub>O relative amount, and CuO thickness, we hypothesize that oxidation of smaller particles does not result in the formation of an oxide shell that reaches a critical stress level needed for nanowire growth [18]. Furthermore, the faster rate of oxidation of smaller particles rapidly depletes the



Cu<sub>2</sub>O shell, thereby eliminating the short-circuit [23] (lower activation energy) diffusion paths needed for nanowire growth.

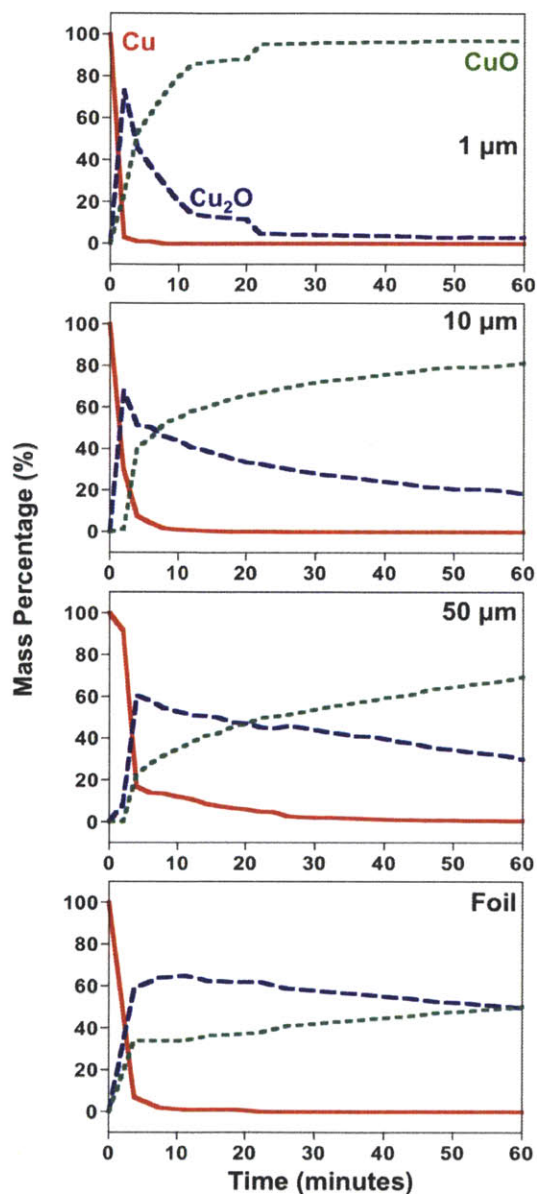


**Figure 5.** In-situ XRD time scans of copper samples revealing a variation in the relative amounts of Cu, Cu<sub>2</sub>O, and CuO with initial particle size. Differences in copper availability and Cu<sub>2</sub>O formation with size are proposed to cause different nanowire growth regimes based on diffusion and stress in the outer oxide shell.

In-situ XRD reveals a dependence of the relative amounts of Cu, Cu<sub>2</sub>O, and CuO on initial particle size. As observed in the TGA experiment, the rate of formation of copper oxide increases with decreasing particle size. Within only the first minute, copper is completely depleted on the 1µm size powder. Likewise, the Cu<sub>2</sub>O phase disappears after 20-30 minutes on the 1µm powder but around 30-60% remains on the larger sizes after the same amount of time.

Based on these XRD results, we explain the size-dependent nanowire growth by looking at the three essential conditions required for nanowire growth: Cu availability, Cu<sub>2</sub>O formation, and CuO thickness. A more rapidly depleted Cu<sub>2</sub>O layer on smaller sized particles combined with copper depletion in the particle core eliminates the possibility for substantial copper diffusion through a defective Cu<sub>2</sub>O layer that was proposed as essential to nanowire formation. Furthermore, we expect that a sufficiently thick CuO layer did not form on the 1µm particles to achieve a critical level of stress that has been suggested [18] for the promotion of nanowires. Using empirical results, an approximate initial particle size necessary to achieve a critical oxide thickness for nanowire growth can be calculated. An upper limit for the CuO oxide shell thickness that can be formed from a copper particle is calculated by considering the limiting case of complete oxidation of Cu to CuO. The relative change in volume resulting from the oxidation is determined from the known molecular mass,  $M$ , and density,  $\rho$ , of the Cu and CuO:

$$\frac{V_{CuO}}{V_{Cu}} = \frac{M_{CuO}/\rho_{CuO}}{M_{Cu}/\rho_{Cu}} = 2.28$$

Here we assume an approximately spherical copper particle of initial radius  $r_i$ . One model [18] of the nanowire formation process involves the diffusion of copper ions through the Cu<sub>2</sub>O and CuO shells to react at the Cu<sub>2</sub>O/CuO interface and the CuO interface with the environment. Since no reaction occurs at the Cu/Cu<sub>2</sub>O interface, the position of the Cu/Cu<sub>2</sub>O interface is expected to remain approximately constant at  $r_i$ . The volume ratio of a copper shell with thickness  $t$  and inner radius  $r_i$  to the initial copper particle of radius  $r_i$  is given by:

$$\frac{V_{CuO}}{V_{Cu}} = \frac{\frac{4}{3}\pi[(r_i + t)^3 - r_i^3]}{\frac{4}{3}\pi r_i^3} = \left(1 + t / r_i\right)^3 - 1$$

By equating the right-hand side of Eq. 1 and 2, we can solve for a lower limit on the radius of the initial copper particle required to obtain a CuO shell of thickness  $t$ . The resulting radius is  $r_i = 2.04t$ , or in terms of the initial particle diameter,  $d_i$ ,  $d_i \approx 4t$ . According to Yuan et al. [18], CuO nanowire growth does not begin until the CuO layer reaches a critical thickness of around  $t_{cr} \approx 1\mu\text{m}$ . Therefore from the above calculation, we predict a cut-off diameter below which there is no appreciable nanowire growth of approximately  $4\mu\text{m}$ . Other papers have reported nanowire growth on flat substrates as thin as  $0.5\mu\text{m}$  [24], and thus the cut-off particle diameter may be as low as around  $2\mu\text{m}$ . The calculated critical oxide thickness for nanowire growth of  $\sim 2\text{-}4\mu\text{m}$  is consistent with our observed results of little to no nanowire growth on  $1\mu\text{m}$  sized particles oxidized at  $600^\circ\text{C}$ . It is expected that the reaction rates are even faster at ambient 21% oxygen, further supporting our observed size-dependent results in Figure 1.

Given our hypothesis of outward copper diffusion from a spherical core and the observation [25] that such a process led to inner pores and void formation in cobalt or nickel-plated beryllium powder, we checked for void formation with a dual-beam focused ion beam (FIB) and SEM (Zeiss NVision 40). After cutting open and imaging the particles, we discovered that the oxidized particles are hollow (Figure 6). In comparison, the unoxidized particles are solid (Figure 7).

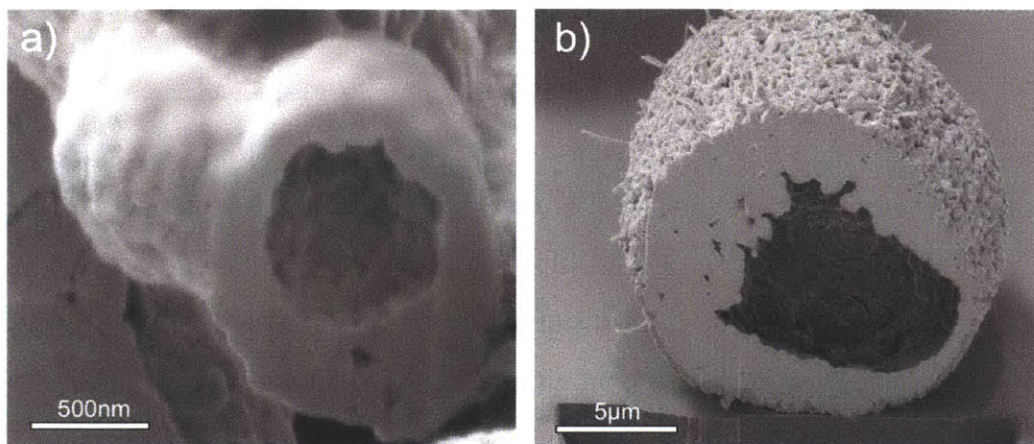


**Figure 6.** SEM images of a FIB-milled cross-section of a 1 $\mu$ m (a) and 10 $\mu$ m (b) oxidized copper particle. These voids are proposed to result from the Kirkendall effect and support a mechanism of outwardly diffusing copper.

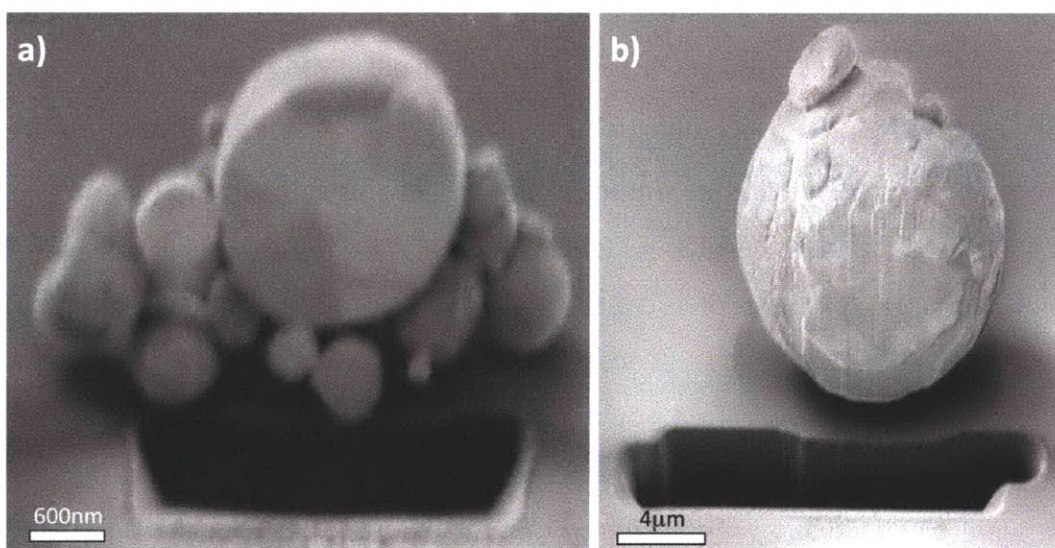


**Figure 7.** FIB control revealing solid cross-sections of an unoxidized a) 1 $\mu$ m and b) 10  $\mu$ m copper particle.

The observed void formation could be explained by the Kirkendall effect, which has been reported to cause voids in the oxidation of cobalt nanoparticles [26]. The preformed surface oxide provides defects for metal-out diffusion from the particle core to the surface region where oxygen anions are relatively immobile [16, 27]. If the inwardly migrating vacancies become supersaturated in the core, then



they coalesce into a single void. For studies [25] on 30 $\mu$ m cobalt or nickel-plated beryllium powder, the Kirkendall effect led to a large volume fraction of pores but without the intact outer shell observed in our samples. Our FIB results confirm the proposed mechanism of outwardly diffusing copper atoms, which leads to the formation of a central void and hollow particles.

## Experimental Methods

*Thermal oxidation:* The samples were prepared by depositing spherical copper powder (99-99.9% metals basis, Alfa Aesar) with an average particle size of 1 $\mu$ m, 10 $\mu$ m, and 50 $\mu$ m on a flat silicon substrate followed by heating for 30 minutes in a box furnace (Thermolyne Benchtop Muffle Furnace, Thermo Fisher Scientific) that was preset to the desired temperature and operated under ambient air in a fume hood. The 1 $\mu$ m and 10 $\mu$ m powder were used as received, and the 50 $\mu$ m powder was sieved to a size range between 45 $\mu$ m and 53 $\mu$ m. The particle size distribution on the 1 $\mu$ m and 10 $\mu$ m powders is as follows: for the 1 $\mu$ m powder, 10% of the particles are at or below 0.47 $\mu$ m, 50% are at or below 0.75 $\mu$ m, and 90% are at or below 1.88 $\mu$ m; for the 10 $\mu$ m powder, 10% of the particles are at or below 7.34 $\mu$ m, 50% are at or below 10.17 $\mu$ m, and 90% are at or below 14.83 $\mu$ m.

*Thermogravimetric analysis:* Thermogravimetric analysis was performed on a TGA Q50 (TA Instruments) at 600°C for 1hr in air. The copper particles were heated to 600°C in nitrogen, and the gas was switched to air to start the oxidation.

*In-situ x-ray diffraction:* A PANalytical X'Pert Pro was used for all experiments. The copper particles were heated to 600°C in nitrogen, and the gas was switched to an atmosphere consisting of 5% oxygen and 95% nitrogen in order to slow down the rate of the reaction and capture the evolution of the initial process. Every two minutes, the copper sample was scanned between 33-45° with each scan taking two minutes to complete. The raw data was analyzed using the High Score Plus software package.

*FIB milling and SEM imaging:* A Zeiss NVision 40 was used to mill and image in-situ the resulting structure. An ion current of 1.5nA at 30kV was used for milling and a finer mill current of 40 pA at 30kV for polishing. The SEM images were taken at 2kV.

## **Applications**

Our results can be applied to sintering, catalysis, chemical looping combustion, and thermal management applications including heat pipes, boilers, and electronics cooling. The size-dependent oxidation could be extended to optimize oxygen carriers in chemical looping combustion. Furthermore, the high surface area of nanowire-covered particles with inner voids might be used to enhance catalytic activity. Size-dependent kinetics is also useful in sintering and the creation of wicking structures where a controllable porosity is desired.

We propose a straightforward process to synthesize new hierarchical structures through a tunable growth process. By mixing small and large particles, wherein smaller particles readily sinter and nanowires grow only on larger particles, we created the hierarchical structures as shown in Figure 8. Such hierarchical structures can be used to improve the wicking ability and fluid transport in heat pipes and enhance boiling heat transfer. With these structures, we have demonstrated *enhanced heat transfer in spray-cooling applications* [8].

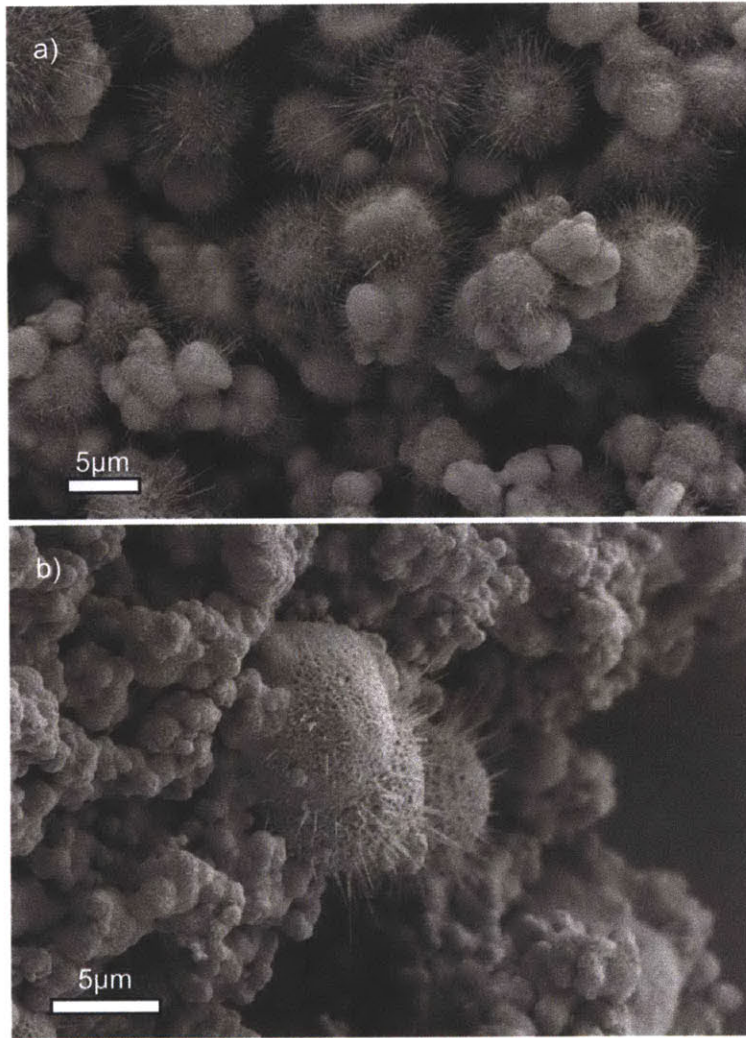


**Figure 8.** Tunable hierarchical structures produced using the size-dependent nanowire growth. a) oxidized at 500°C for 30 minutes and b) 600°C for 15 minutes. Differences in sintering and nanowire growth are demonstrated with mixed particle sizes. Smaller particles readily sinter while nanowires grow only on larger particles.

Spray cooling is capable of high heat transfer by the phase-change of liquid droplets impacting a heated surface. The main components of a typical system are a nozzle and pump. In addition to high heat removal, spray cooling can provide relatively uniform surface temperature over large areas and no temperature overshoot characteristic of boiling incipience [29]. Spray cooling has been most commonly used in continuous metal casting, nuclear reactor safety systems, and

food processing. Under continued development is the application of spray cooling for electronics [29].

An important parameter affecting the performance of a spray-cooling system is the Leidenfrost temperature. The Leidenfrost temperature marks the transition between the nucleate and filmwise boiling regimes (Figure 9a). Nucleate boiling is visibly characterized by droplet surface wetting, whereas filmwise boiling occurs when the liquid drop is suspended above the surface on a layer of its own vapor (Figure 9b). In a cooling application, nucleate boiling is preferred for higher heat transfer coefficients (up to an order of magnitude).

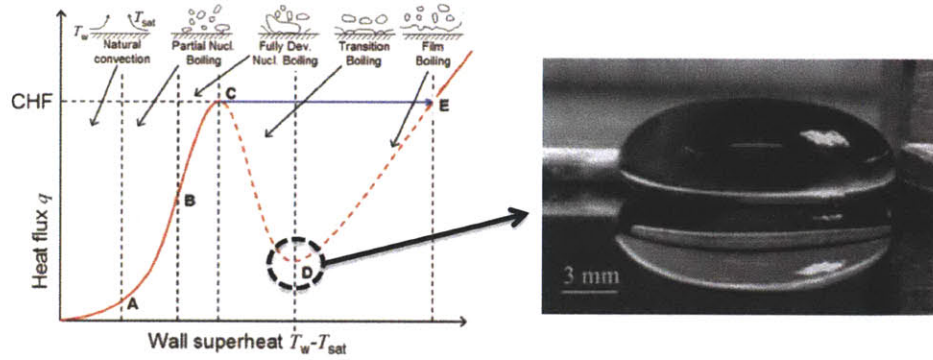


**Figure 9.** a) Standard pool boiling curve with the Leidenfrost temperature indicated by the circled point D [reprinted from Ref. 13]; b) Leidenfrost droplet on a heated silicon surface [reprinted from Ref. 28].

## Leidenfrost Experiments

The spray-cooling performance of a new hierarchical coating was investigated and compared to a conventional flat substrate (silicon) by measuring the Leidenfrost temperature. The hierarchical coatings are made by first using a doctor blade to uniformly spread the copper powder across the substrate at a preset desired thickness of around 100 $\mu\text{m}$  (Figure 10a). Then the thermal oxidation process described in this thesis forms the resulting hierarchical structure consisting of spherical particles (average diameter of 50 $\mu\text{m}$ ) with nanowires protruding



outward from the surface. While systematically testing the performance of flat hierarchical substrates, we are simultaneously investigating the modification of traditional manufacturing processes—such as layer-by-layer, powder spray, and powder metallurgy (Figure 10b) —to coat a variety of geometries including tubes.

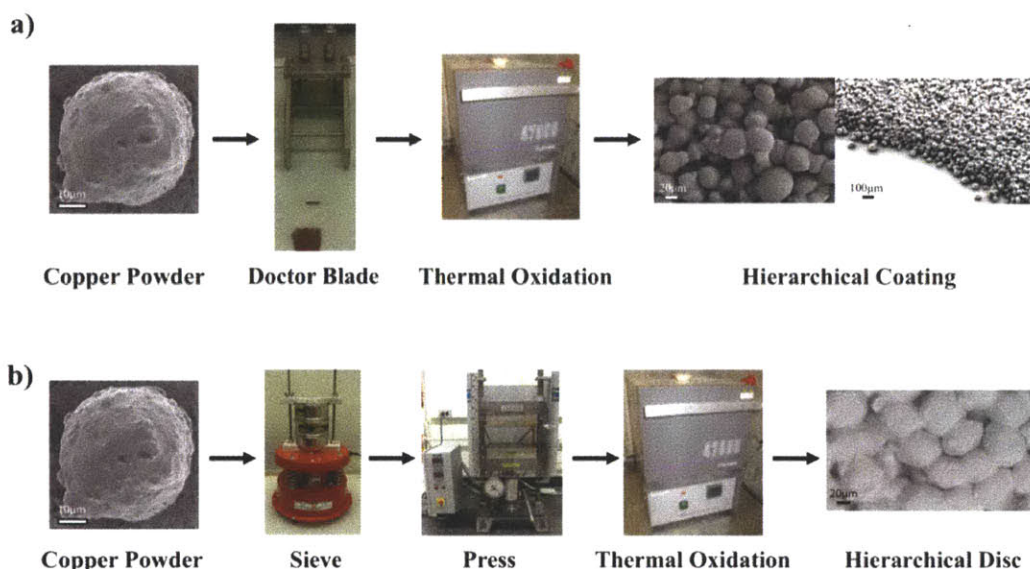


**Figure 10.** a) Doctor blade method followed by thermal oxidation to form flat, uniform hierarchical coating b) Modification of powder metallurgical process to form porous copper hierarchical disc structure

The Leidenfrost temperature was determined by heating the surfaces to a given temperature (measured with a thermocouple) and recording the interaction of a water droplet with the surface using a high-speed camera. The water droplet was initially subcooled (at room temperature) and gently deposited on the surface. The temperature between droplet wetting and nonwetting on the heated surface is the Leidenfrost temperature. Since the drop is initially subcooled, in some instances boiling may occur when the drop re-interacts with the surface after initially being repelled away from it. If the drop doesn't boil after the first couple of bounces, then we consider it to be a Leidenfrost drop.

The Leidenfrost temperature of a flat silicon surface was found to be around 280°C (Figure 11a). At the same temperature, water still undergoes nucleate boiling on the hierarchical coating and the substrate is below its Leidenfrost temperature.

The surface temperature of the hierarchical coating was increased up to the limit of the heating system. Even at a temperature of  $\sim 90^\circ\text{C}$  higher than the flat substrate, water still undergoes nucleate boiling and the Leidenfrost temperature hasn't been reached (Figure 11b).

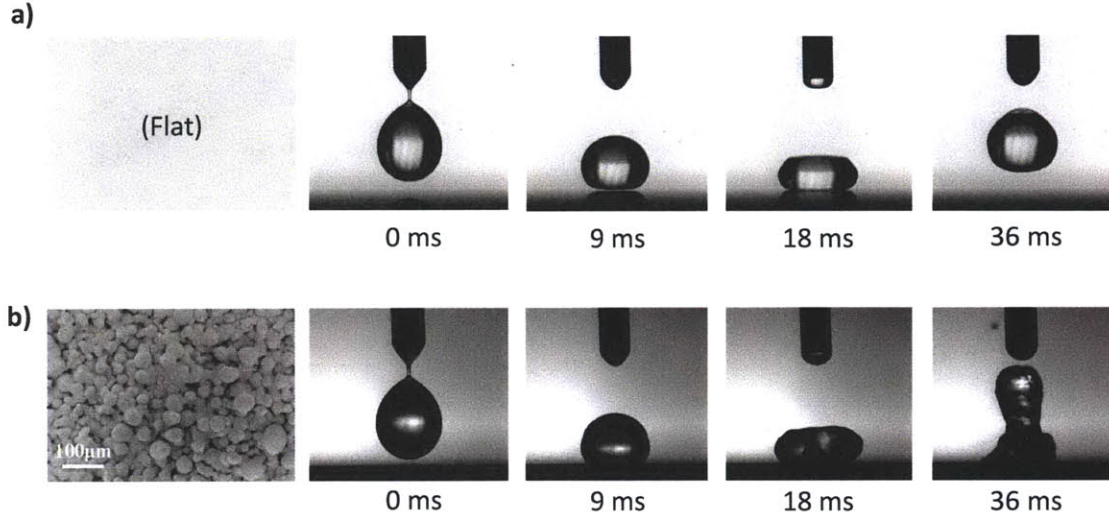


**Figure 11.** a) Leidenfrost water droplet on a flat silicon surface at  $\sim 280^\circ\text{C}$ ; b) water nucleate boiling at  $\sim 370^\circ\text{C}$  on a hierarchical coating (below Leidenfrost temperature).

We propose that this remarkable increase in spray-cooling performance is due to the unique geometry of the hierarchical coating. First of all, the nanowires and surface roughness make the coating superhydrophilic (contact angle of  $\sim 0^\circ$ ), and the nanotexture may also promote droplet wetting by the addition of a capillary pressure, which is a difference in pressure across the liquid-vapor interface. For a given feature with surface energy,  $\gamma$ , and radii of curvature,  $R_1$  and  $R_2$ , the capillary pressure,  $\Delta P$ , is given by the Young-Laplace equation:

$$\Delta P = \gamma \left( \frac{1}{R_1} + \frac{1}{R_2} \right).$$

Therefore, as the surface feature size decreases, the capillary pressure increases and surface rewetting is expected to be enhanced. However, there is a

competing effect with reducing capillary size; the vapor permeability decreases and an optimum may be reached between increased surface rewetting and flow of newly created vapor out of the texture. This result can be seen mathematically by considering the general case of flow through porous media (Darcy's Law):

$$Q = \frac{kA}{\mu L} \Delta P,$$

where  $Q$  is the flow rate,  $k$  is the permeability,  $A$  is the cross-sectional flow area,  $\mu$  is the fluid viscosity,  $L$  is the length along the flow, and  $\Delta P$  is the pressure drop (given above by the Young-Laplace equation). As the feature size of the texture decreases, the permeability decreases and vapor flow away from the surface is more difficult. If the vapor is more easily trapped within the surface textures, then the transition to filmwise boiling will occur and the beneficial effects of increased surface wettability are cancelled out.

A hierarchical coating overcomes the drawbacks of a conventional nanotexture-only surface by incorporating the nanotexture over a larger length-scale structure that allows for both high liquid wettability and vapor permeability. Though typically difficult to form a hierarchical coating, this thesis presents a new method that is simple and scalable based on the size-dependent thermal oxidation of spherical copper powder. In the future, we plan to systematically study the competing effects of capillarity and permeability and determine the optimal hierarchical parameters to achieve the highest Leidenfrost temperature.

## Conclusion

This thesis presents a new discovery of a size-dependent thermal oxidation of spherical copper powder. There is a regime of around  $3\mu\text{m}$  and below with no appreciable nanowire growth and a regime of around  $10\mu\text{m}$  and above where the particles are mainly covered by straight and non-branching wires that grow perpendicular to the surface. Systematic thermogravimetric analysis (TGA) and in-situ x-ray diffraction (XRD) studies of the thermal oxidation of particles of different sizes provide insights into the size-dependent process and evolution of the various

phases of copper and copper oxide with time. Furthermore, it has been shown that these particles are hollow after oxidation and this observation is consistent with our proposed mechanism based on outward copper diffusion. In a simple and single-step process, solid spherical powder is converted to very rough hollow spheres with nanowires protruding from their surface.

The control of nanowire formation can be used to create new hierarchical coatings. The application of these coatings to spray cooling revealed substantial improvements over a conventional flat surface. I anticipate future advances in thermal management based on applications of this new scalable manufacturing method and the use of hierarchical surface structures.

## Bibliography

- [1] K. Koch, *et al.*, "Fabrication of artificial Lotus leaves and significance of hierarchical structure for superhydrophobicity and low adhesion," *Soft Matter*, vol. 5, pp. 1386-1393, 2009.
- [2] C. Neinhuis and W. Barthlott, "Characterization and distribution of water-repellent, self-cleaning plant surfaces," *Annals of Botany*, vol. 79, pp. 667-677, 1997.
- [3] X. Gao and L. Jiang, "Water-repellent legs of water striders," *Nature*, vol. 432, p. 36, 2004.
- [4] D. Sen and M. J. Buehler, "Structural hierarchies define toughness and defect-tolerance despite simple and mechanically inferior brittle building blocks," *Nature Scientific Reports*, vol. 1, pp. 1-9, 2011.
- [5] H. E. Jeong, *et al.*, "UV-assisted capillary force lithography for engineering biomimetic multiscale hierarchical structures: From lotus leaf to gecko foot hairs," *Nanoscale*, vol. 1, pp. 331-338, 2009.
- [6] W. Ming, *et al.*, "Superhydrophobic Films from Raspberry-like Particles," *Nano Letters*, vol. 5, pp. 2298-2301, 2005.
- [7] C. J. Love, *et al.*, "Hierarchical Nanostructures by Thermal Oxidation of Metals," US Patent, 2011.
- [8] HyukMin Kwon, *et al.*, "Superwetting surfaces for diminishing Leidenfrost effect,



- methods of making and devices incorporating the same," US Patent, 2010.
- [9] K. K. Varanasi, *et al.*, "Articles Having Enhanced Wettability," US Patent, 2006.
- [10] G. P. Peterson, *An introduction to heat pipes: modeling, testing, and applications*: John Wiley & Sons, Inc., 1994.
- [11] J. A. Weibel, *et al.*, "Characterization of Evaporation and Boiling from Sintered-Powder Wicks Fed by Capillary Action," *International Journal of Heat and Mass Transfer*, vol. 53, pp. 4204-4215, 2010.
- [12] M. A. Hanlon and H. B. Ma, "Evaporation Heat Transfer in Sintered Porous Media," *Journal of Heat Transfer*, vol. 125, pp. 644-652, 2003.
- [13] R. Chen, *et al.*, "Nanowires for Enhanced Boiling Heat Transfer," *Nano Letters*, vol. 9, pp. 548-553, 2009.
- [14] C. Li, *et al.*, "Nanostructured Copper Interfaces for Enhanced Boiling," *Small*, vol. 4, pp. 1084-1088, 2008.
- [15] S. G. Liter and M. Kaviany, "Pool-boiling CHF enhancement by modulated porous-layer coating: theory and experiment," *International Journal of Heat and Mass Transfer*, vol. 44, pp. 4287-4311, 2001.
- [16] C. H. Xu, *et al.*, "Formation of CuO nanowires on Cu foil," *Chemical Physics Letters*, vol. 399, pp. 62-66, 2004.
- [17] X. Jiang, *et al.*, "CuO Nanowires Can Be Synthesized by Heating Copper Substrates in Air," *Nano Letters*, vol. 2, pp. 1333-1338, 2002.
- [18] Lu Yuan, *et al.*, "Driving force and growth mechanism for spontaneous oxide nanowire formation during the thermal oxidation of metals," *Acta Materialia*, vol. 59, pp. 2491-2500, 2011.
- [19] Y. W. Park, *et al.*, "Growth Mechanism of the Copper Oxide Nanowires from Copper Thin Films Deposited on CuO-Buffered Silicon Substrate," *Journal of The Electrochemical Society*, vol. 157, p. K119, 2010.
- [20] A. M. B. Gonçalves, *et al.*, "On the growth and electrical characterization of CuO nanowires by thermal oxidation," *Journal of Applied Physics*, vol. 106, p. 034303, 2009.
- [21] L.S. Huang, *et al.*, "Preparation of large-scale cupric oxide nanowires by thermal evaporation method," *Journal of Crystal Growth*, vol. 260, pp.130-135, 2004.

- [22] J.T. Chen, *et al.*, "CuO nanowires synthesized by thermal oxidation route," *Journal of Alloys and Compounds*, vol. 454, pp. 268-273, 24 April 2008.
- [23] Robert W. Balluffi, *et al.*, "Kinetics of Materials," in *Kinetics of Materials*, New Jersey: John Wiley & Sons, Inc., 2005.
- [24] N. J. S. Yeon-Woong Park, Hyun-June Jung, Anupama Chanda, Soon-Gil Yoon, "Growth Mechanism of the Copper Oxide Nanowires from Copper Thin Films Deposited on CuO-Buffered Silicon Substrate," *Journal of The Electrochemical Society*, vol. 157, pp. K119-K124, 2010.
- [25] F. Aldinger, "Controlled Porosity by an Extreme Kirkendall Effect," *Acta Metallurgica*, vol. 22, pp. 923-928, 1974.
- [26] Y. Yin, "Formation of Hollow Nanocrystals Through the Nanoscale Kirkendall Effect," *Science*, vol. 304, pp. 711-714, 2004.
- [27] Y. Chang, *et al.*, "Large-Scale Synthesis of High-Quality Ultralong Copper Nanowires," *Langmuir*, vol. 21, pp. 3746-3748, 2005.
- [28] A. Biance, *et al.*, "Leidenfrost Drops," *Physics of Fluids*, vol. 15, pp. 1632-1637.
- [29] A. Bar-Cohen *et al.*, "Direct Liquid Cooling of High Flux Micro and Nano Electronic Components," *Proceedings of the IEEE*, vol. 94, pp. 1549-1570.